J. Fluid Mech. (1975), *vol.* 72, *part* 1, *pp.* 35–47
Printed in Great Britain

Some experiments on the motion of an isolated laminar thermal

By D. J. SHLIEN† AND D. W. THOMPSON
Department of Chemical Engineering, University of British Columbia, Vancouver

(Received 6 August 1974 and in revised form 18 April 1975)

A novel technique for injecting buoyancy (heat) into a liquid is described and demonstrated. When buoyancy was injected for a short time a laminar vortex ring formed. Its vertical displacement was found to be only approximately proportional to the square root of time (measured from an apparent initial time). Approximate geometrical similarity was also observed although the Reynolds number decreased from 28 to about 14.

1. Introduction

Perhaps the most fundamental phenomenon occurring in convective heat (or mass) transfer problems is the motion resulting from heat (or buoyancy) released from a point source in a stationary infinite fluid. It is fundamental to problems over a large range of Rayleigh numbers. In the atmosphere the phenomena of plumes (continuous injection of heat) and thermals (release of heat over a short period of time) occur. Examples of plumes are the smoke emitted from chimneys and heat released from large cooling towers. Thermals were first noticed (and named) by glider pilots although birds which fly long distances have always used them to gain altitude with minimum effort. Smaller Rayleigh number thermals have been observed in heat transfer from a heated flat plate to a fluid. Elder (1967, 1968, 1969) appears to be one of the first to have observed this visually (in a porous medium), followed by Sparrow, Husar & Goldstein (1970). Thermals have also been observed in experiments on ice formation (Tankin & Farhadieh 1971) and in gas absorption in pools of liquid (Thompson 1970). Chu & Goldstein (1973) concluded that, at least in the overall Rayleigh number range 10^5–10^7, "the main heat transfer mechanism (for a heated horizontal plate) is the release of thermals".

The applications of this fundamental problem are both broad and varied, ranging from heat-transfer to pollution problems, to cloud formation and seeding, electro-plating, orchard heating for frost protection and to defence applications. Yet the problem has by no means been completely solved.

In this paper, some aspects of the formation, growth and motion of laminar thermals are described. Although no new theories are presented, some rough explanations of the observations are given. Similarity is investigated and the effect of the Rayleigh number on the convection velocity is estimated from the

† Present address: School of Engineering, Tel-Aviv University, Israel.

data. It is hoped that the observations described in this paper will lead to improved theories.

For laminar thermals, no measurements and very few analyses have been found in the literature although there are a considerable number of papers dealing with the turbulent case. Since there are features common to both,† investigations of turbulent thermals are mentioned briefly.

Taylor (1946) was one of the first to examine the dynamics of thermals. By considering the gross governing equations and assuming that the influx of fluid into the thermal is proportional to the convection velocity, he derived the relations $d \propto y \propto Q^{\frac{1}{4}}t^{\frac{1}{2}}$ for turbulent thermals, where y, t and d are the thermal's height from the source, time from injection and diameter respectively and Q is the total heat contained in the thermal. This was followed by other approaches and extensions by Batchelor (1954), Morton, Taylor & Turner (1956), Scorer (1957), Turner (1957, 1964), Wang (1971) and Escudier & Maxworthy (1973). In addition to the experiments conducted by some of these authors, measurements were made by Woodward (1959), Richards (1961), Turner (1963), Fohl (1968) and Lin, Tsang & Wang (1972). Numerical integrations of the governing equations were attempted by Malkus & Witt (1959), Ogura (1962), Lilly (1962, 1964) and Fox (1972). Fox considered the three-dimensional case in the hope of observing a range of thermals from stable laminar ones to turbulent ones. Unfortunately he was not able to reach a high enough Reynolds number to obtain unstable flows.

Most, if not all, laboratory-generated thermals reported in the literature had irregular, cauliflower-like surfaces. It is believed by the authors that in many cases the form of the irregularities (and possibly the gross features) may have been strongly affected by the injection method. Also since a transition Rayleigh number is yet to be found, one cannot be certain that the thermals were truly turbulent. One of the major experimental difficulties is construction of a sufficiently small buoyancy source to avoid lateral structure such as that observed with a heated horizontal plate.

To the authors' knowledge, the only analysis of laminar thermals in the literature is by Morton (1960), who obtained a similarity solution to the governing equations (under the Boussinesq approximation) up to first order in an effective Rayleigh number A_m. The resulting laminar flow pattern was similar to that for an ordinary vortex ring and the temperature field was similar to that in a solid (no concentration of heat in the core of the vortex ring). Similarity was found to require that the ratio d^2/t be constant. The solution for a Prandtl number of unity gave $y = (A_m/12\pi)(Dt/\pi)^{\frac{1}{2}}$ and $d = 3{\cdot}02(2Dt)^{\frac{1}{2}}$, where $A_m \equiv \beta g Q/\rho c D\nu$, β is the coefficient of thermal expansion, D is the thermal diffusivity, and ν is the kinematic viscosity. The results for this 'weak thermal vortex ring' (laminar) differ from previous ones (turbulent) in the dependence of y on Q.

† Dimensionally, laminar flows involve an additional parameter compared with turbulent flows (for gross features of the flow), namely the kinematic viscosity.

2. Apparatus and experimental technique

Odell (1971, private communication) suggested a novel way of injecting heat into a liquid: by operating a 'single-electrode' conductivity probe (Gibson & Schwarz 1963) at high power. The advantages of this technique are as follows.

(i) The fluid is heated directly, without the need for an intermediate *heating element*, which causes transients owing to its finite heat capacity. Unfortunately, in the present application, the electrode, having a thermal conductivity of about 130 times that of the liquid, introduced transients because of heat conducted *from* the liquid *to* the electrode.

(ii) Accurate measurement of the buoyancy input is possible.

(iii) Buoyancy can be injected in a single pulse, periodic pulses or continuously.

(iv) The geometry of the heat source can be easily altered.

Some experiments employing this technique will be described. Also, a 16 mm motion picture demonstrating these phenomena is available from either of the authors. The technique may also be useful for heat-transfer and boiling studies and for modelling physical systems such as heat discharge from power stations.

The experiments were conducted in a glass vessel $12{\cdot}0 \times 11{\cdot}7$ cm in cross-section and about 20 cm high filled to 2 cm from the top with a 27 % sodium carbonate solution. A closely fitting lid was necessary to prevent evaporative convection which could otherwise be seen in a shadowgraph. Heat was injected into the solution by passing a 10 kHz current from a small electrode (0·80 mm diameter wire with only the tip uninsulated) to a large one (approximately 4×6 cm). Only the solution very close to the small electrode was heated since the current density was large there. The electrode tip was located at about 6 cm from the bottom of the vessel.

A 10 kHz (to prevent electrolysis) sine wave form was passed through a switching circuit driven by a low frequency square wave which effectively gated the sinusoid on and off. This signal was amplified in amplitude and power and then connected to the electrodes. The power input into the fluid was determined by turning off the switching circuit and then measuring the r.m.s. voltage and current with a Marconi digital multimeter (model 270). The power factor was very close to unity (0·995).

The thermals and plumes were made clearly visible using shadowgraph techniques (figure 1). The pencil of light from a Spectra-Physics helium–neon laser (model 124 A, 15 mW) was redirected by two front-surface mirrors, then filtered, expanded and collimated to 2·5 cm or 5·0 cm beams using a Spectra-Physics 332 spatial filter and a Spectra-Physics 331 or 333 collimating lens. After passing through the glass container, the beam was expanded and then allowed to fall on a 75 cm square back-projection screen. The image on the screen was filmed on 16 mm Kodak 4-X negative 7224 film rated at 400 ASA with a Bolex H16 reflex cine camera at a framing rate of 11 frames/s. The timing was determined by double exposing the shadowgraph film with the digits of a Monsanto counter (model 100 B), counting a 1 kHz signal. This method gave repeatable timing to within 1 % over one day.

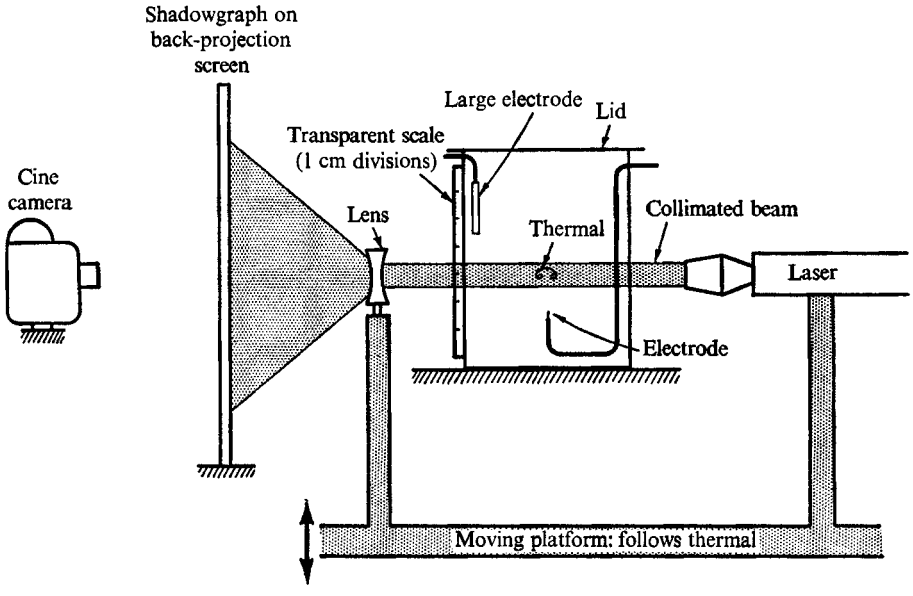

FIGURE 1. Apparatus.

The laser and optics were mounted on a large tripod to follow (manually) the motion of the thermal or plume. The relative location of the thermal was determined to within approximately 0·07 mm by mounting a transparent scale on the tank so that the light beam passed through it and projected the graduations on the screen. The film was viewed and measured using a Specto Motion Analysis Projector MK III.

After setting the voltage for the required power input and setting the timing of the switching circuit, the solution in the glass container was stirred for about 10 min using a Cenco magnetic stirrer. The solution was then allowed to settle for 1–2 h before starting the experiment. Directly after each run, the energy input was checked and the film double exposed for the timing. The room temperature typically remained constant to within about 1 °C over one day.

Several difficulties were encountered which might interest those wishing to use this technique. Occasionally electrolysis would occur, for no apparent reason. It is suspected that the electrode (platinum) somehow became fouled. A more serious problem was the difficulty in obtaining repeatable results (the deviation in the displacement after 50 s was as much as 5 % in one case). This is not thought to be due to any lack of precision in measuring and setting the energy input. A possible cause might be changes in ambient density from one run to the next† (a result of changes in room temperature or changes in concentration resulting from filtering the solution with the aid of a vacuum pump).

† Dimensional analysis with the parameters y, t, Q, τ (injection time duration), g, ρ_0, ν, D, β and c requires that Q and ρ_0 appear in the ratio Q/ρ_0 since the dimension of mass occurs *only* in these parameters. Thus a change in the ambient density ρ_0 can be thought of as an effective change in the amount of injected heat Q. However, Maxworthy (1974, private communication) estimated that a 3 °C temperature change would result in about a 3 % change in the rise height owing to the variation of viscosity with temperature.

Sparrow *et al.* (1970) found that measurable changes in the frequency of thermal shedding from a heated plate resulted from changes in the fluid temperature of 3 °C with the temperature difference between the plate and fluid held constant. This change in ambient density (or temperature) probably resulted in a level change of the displacement curve, as in runs 2903*L* and 2903*K* (see figures 3 and 4 below). Small stratification, on the other hand, most likely altered the curve shape (runs 2303*I* and 2303*K*, same figures). To be more certain of the results, each experiment was repeated several times. The degree of repeatability obtainable is apparent in the $A_m = 9600$ data (same figures).

Besides the motion pictures previously mentioned, sequences of still photos were taken using a motorized Nikon 35 mm camera with a 0·001 s exposure. The camera, with its lens and viewing prism removed, was mounted in the position of the expanding lens. The resulting photos, some of which are presented here, were much clearer than those taken using other techniques.

In all measurements presented here the time interval τ over which heat was injected was 0·667 s. Variation of τ from 0·3 to 1·0 s while keeping the total heat injected constant seemed to have only a small effect on the thermal displacement.

3. Development of thermal vortex rings

A sequence of photos showing the motion and growth of a thermal vortex ring ($A_m \approx 9600$) is shown in figure 2 (plate 1). These were taken with the motorized Nikon 35 mm camera, as described previously. Although the majority of the photos are from one run, three runs were actually performed.† Each photo in a row is aligned to show the actual vertical displacement. A datum line is also shown for each row. For interpretation of the photos, the reader is reminded that the white areas roughly represent maxima in the second derivative of the temperature and the black areas minima. In addition, interference fringes are clearly visible. The first photo (0 s) shows the electrode, for reference.

In the initial stage of injection, the heat is diffused by conduction. This is characterized by a spherical distribution of heat as in the photo at 0·35 s. Convection is estimated to begin at $\sim$ 0·3 s.

After 0·67 s heat was no longer injected, yet the heated fluid can be seen to have been in contact with the electrode for several seconds. This must result from the no-slip boundary condition and heating of the electrode by the fluid in its vicinity. Notice the apparent increased size of the electrode at 1·4 s compared with that at 0 s. The tail or column behind the vortex ring can also be observed in Okabe & Inoue's (1961) photographs, Richard's (1963) experiments (turbulent), Fox's (1972) numerical calculations and in Maxworthy's (1972) experiments with non-buoyant vortex rings. It is also observable in thermals generated by heating a horizontal plate (see, for example, Elder 1969).

The formation of the vortex ring begins with the appearance of a lobe on the vertical boundary (visible in the 0·9 s photo and more obvious in the 1·0 s one).

† The 0·6 and 1·0 s photos are part of one run, those from 20·5 s to the end from a second run and the rest of the photos from the main run.

The lobe must result from the fluid in the centre rising faster than that at the edges. Since the heated fluid displaces ambient fluid from its path and in turn is displaced upwards by ambient fluid at approximately its own level a circulation pattern is set up (as described by Morton 1960). Ambient fluid enters at the inner edge of the trailing end of the lobe as indicated by the white lines demarcating the lobe. This fluid appears to be swept into the lobe (2·3 s photo), causing a decrease in the height-to-width ratio of the thermal. Ambient fluid appears to enter only at the rear of the thermal, contrary to observations of turbulent thermals (Woodward 1959).

As the thermal rises the column seems to stretch (notice the 'necking' at 1·4 s) and diffuse. The core of the vortex ring first appears in the 2·8 s photo, becoming more distinct with time. It is assumed that the core coincides with the dark spot, a minimum in the second derivative of the temperature. The 'cap' of the thermal diffuses slowly with time, probably because gradients in velocity maintain temperature gradients (while thermal conduction reduces them), so that as the thermal's velocity decreases the gradients also decrease, allowing the 'cap' to diffuse. The similarity between thermals and spherical cap bubbles can be seen by comparison of these photos with figure 6 of Wegener & Parlange's (1973) article.

Comparison of these photographs with, for example, Fox's (1972) temperature distributions is very difficult because of problems with the quantitative interpretation of shadowgraphs. However, the shape of the steady temperature distribution in Fox's paper (see especially his figure 3) is very similar to that in the early formation stages of a thermal generated from a point source on a boundary.

The thermal vortex ring appeared to be very stable. Small disturbances to the ambient fluid did not alter its general character.

4. Thermal displacement

In figure 3, the displacement $y(t)$ of the thermal vortex ring as a function of time is plotted for three effective Rayleigh numbers: A_m = 9600, 4800 and 3200.† The displacement y was measured from the tip of the electrode to the core of the thermal. Boiling limited the maximum heat input while the lower limit was chosen such that the thermal would be visible for at least a half minute.

The curves drawn represent $y^2 = k\Delta t$, where Δt denotes time measured from an apparent initial time obtained by plotting y^2 as a function of time. The constant of proportionality k was determined from a plot of $y^2/\Delta t$ as a function of time (figure 4), where only one apparent initial time was required for each A_m (the apparent initial time decreased from 2·3 to 1·0 s with increasing A_m).

The precision of the data fit to $y^2 = k\Delta t$ is more apparent from a plot of $y^2/\Delta t$ as a function of time. These data indicate that, although the fit is close in the range approximately 5–30 s, the deviations are beyond the scatter. For

† The total heat inputs corresponding to these are 0·667, 0·333 and 0·220 cal.

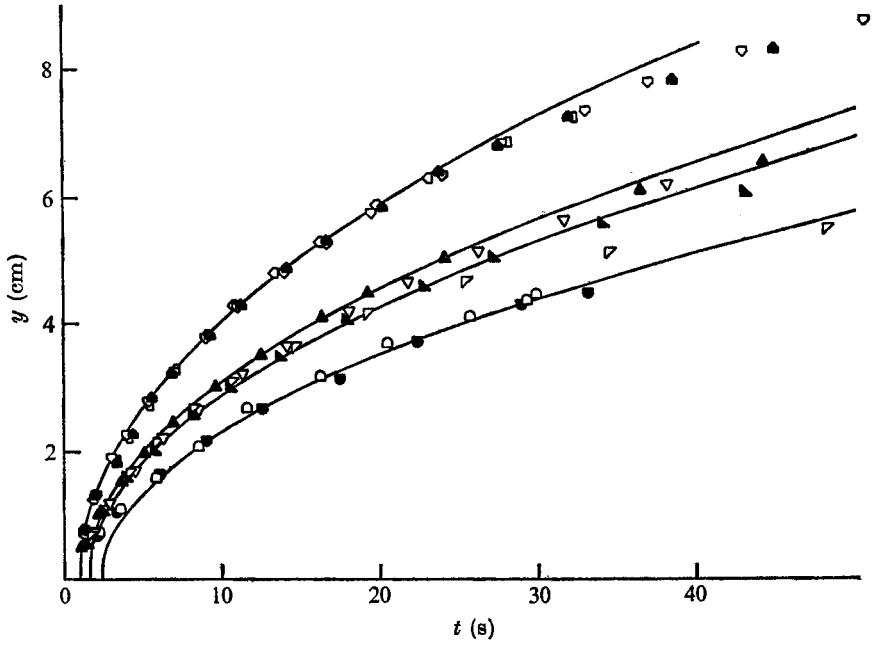

FIGURE 3. Thermal displacement. Curves drawn to fit $y \propto \Delta t^{\frac{1}{2}}$. Runs with $A_m = 9600$: ◁, 0104*M*; ◮, 0104*O*; ▽, 0104*P*. Runs with $A_m = 4800$: ▽, 2303*I*; ▻, 2303*J*; ▲, 2903*L*; ◣, 2903*K*. Runs with $A_m = 3200$: ▢, 2203*F*; ■, 2303*H*.

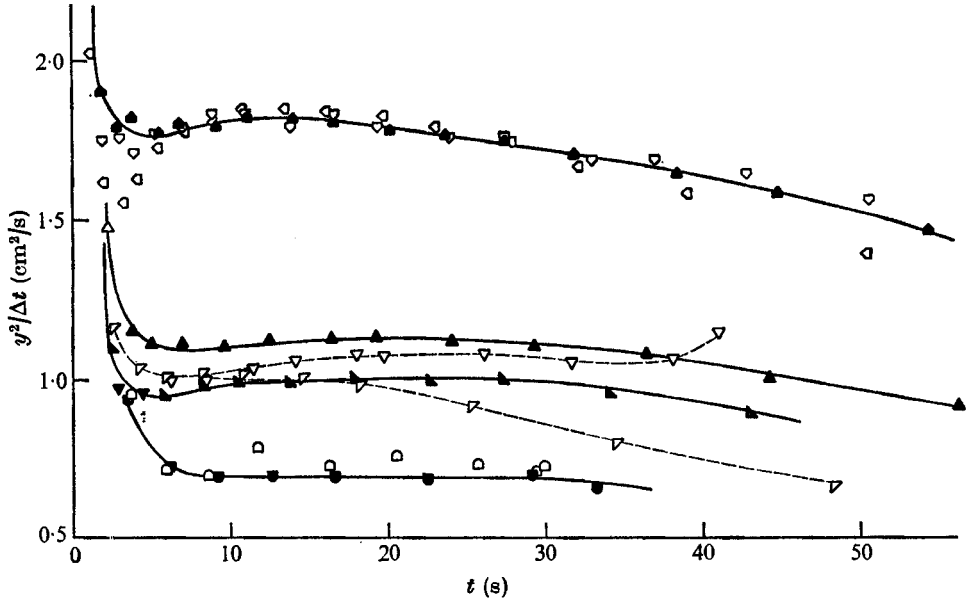

FIGURE 4. $y^2/\Delta t$ as a function of time. Symbols as in figure 3.

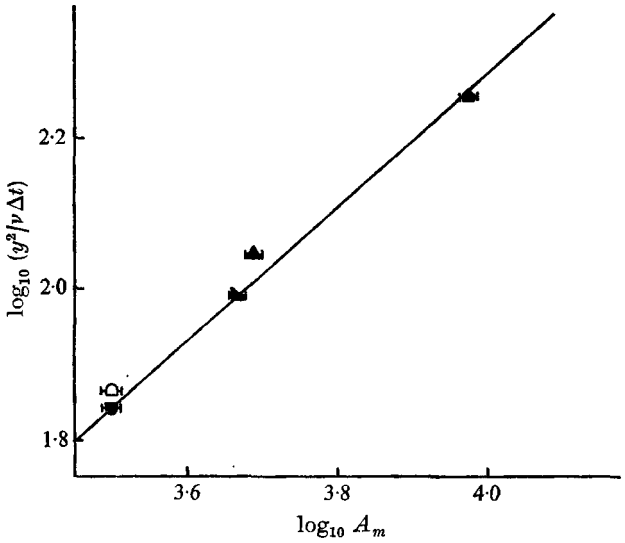

FIGURE 5. Effect of Rayleigh number on displacement. Symbols as in figure 3.

small times the form of the deviation depends strongly on the choice of the apparent initial time. The deviation at small times is to be expected since the thermal vortex ring is in a formation stage and thus similarity should not occur. The deviation at large times may be a result of the dominance of thermal conduction in reducing the temperature gradients over the velocity gradients, which tend to maintain the temperature gradients. For the case $A_m = 9600$, the close proximity of the thermal to the free surface (about two thermal diameters at 30 s) could also contribute to this deviation.

Another possible explanation for the deviation from the $y^2 = k\Delta t$ law is that it assumes that all the runs were performed in a similar (stably) stratified environment. This is very unlikely since the solution was stirred before each run and thus the probability of identically stratified conditions in the repeated runs should be very low indeed. The odd behaviour of runs 2303*I* and 2303*J* can, however, be attributed to stratification and/or fouling of the electrode. Run 2303*F* exhibits considerably more scatter than those at higher Rayleigh numbers, since in some cases it was difficult to see the low Rayleigh number thermals.

An estimate of the effect of the effective Rayleigh number A_m (or the total heat input) on the motion of the thermal is obtained from a plot of the constant k as a function of A_m. In figure 5, a straight line of slope 0·9 has been fitted† to the logarithm of the data. A slope of unity is possible, but 2 or 0·5 seems unlikely. Most authors, starting with Taylor (1946), have predicted 0·5 for turbulent thermals while Morton (1960) predicted 2·0 for weak (laminar) thermals. Maxworthy (1974, private communication) extended his (1972) theory for laminar vortex rings to thermals and obtained a slope of unity. Thus a possible

† Little weight was assigned to the point corresponding to run 2203*F* since its data show considerably more scatter on the $y^2/\Delta t$ plot than the 2303*H* data.

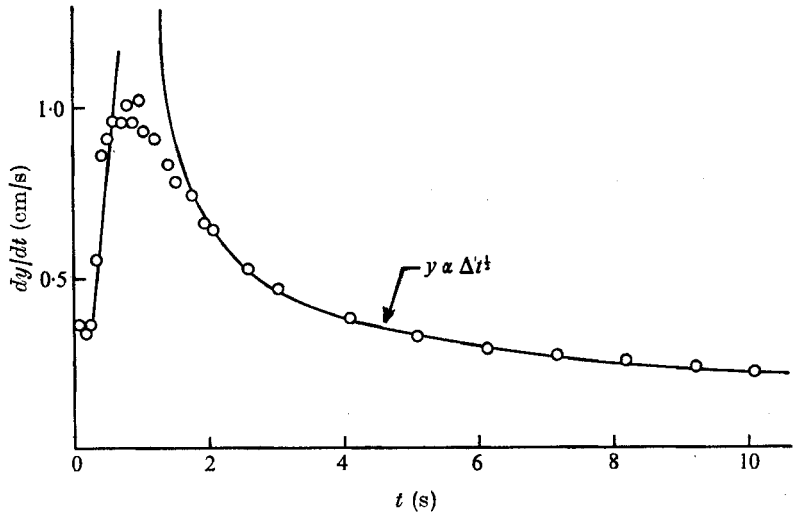

FIGURE 6. Thermal velocity.

equation for the thermal height may be $y \propto \Delta t^{\frac{1}{2}} A_m^a f(P_r)$, where $P_r = \nu/D$ and $a = 2$, 0·9 or 0·5 depending on the Rayleigh number.

Caution is required in the acceptance of a slope of 0·9. The effective Rayleigh number was computed from the total heat injected into the fluid. This includes a considerable amount of heat which is 'left behind' in the tail or column and 'attached' to the electrode. Only if it is assumed that a constant percentage of the heat (independent of A_m) is left behind can this slope be accepted. Furthermore, there is considerable uncertainty in the value of k (indicated by the spread of the pairs of points for lower values of A_m) caused by changes in the ambient density, mentioned previously.

For illustrative purposes, the velocity is plotted as a function of time in figure 6. An initial acceleration period is evident (acceleration $\approx 1{\cdot}8$ cm/s^2). As soon as the heat injection is stopped, the deceleration phase begins. The deceleration appears to be approximately constant until the $y^2 \propto \Delta t$ fit takes over. However, more accurate measurements are required to verify these estimates.

5. Geometric similarity

The law $y^2 \propto \Delta t$ has been shown by Morton (1960) to be a necessary condition for similarity. It should therefore be interesting to check for geometrical similarity. In figure 7 ratios of overall dimensions obtained from measurements of the still photos in figure 2 and the cine film are plotted. The still photos were clearer in most cases, but the time had to be determined from the thermal's position using other measurements of $y(t)$.

Approximate geometric similarity is evident beyond 8 s. The features corresponding to the dimensions b and c were very difficult to see after 20 s, so that the curve after this time is shown as a broken line. Vertical bars near $t = 4$ s

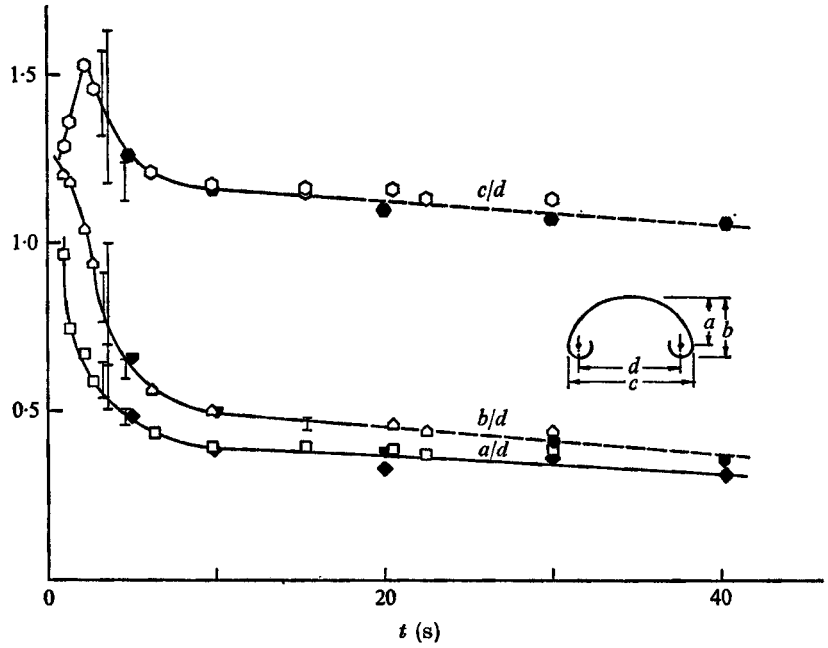

FIGURE 7. Geometric similarity. Open symbols, photos; filled symbols, run 1704C.

indicate the large range of diameters possible since for small times the core was not visible (and perhaps did not exist).

In figure 8 the ratio d/y can be seen to be constant to within approximately 3% for each run (except for the data from the photos). The large deviation of the photo data must indicate a 'poor run'. The three other sets of data deviate slightly from each other. Besides different ambient densities and temperatures, this could have been caused by slight deviations in the setting of the total heat input. For the lower effective Rayleigh numbers, the ratio d/y is estimated to be approximately 0·2. Scorer (1957) obtained 0·7–0·4 with an average of 0·5 in his (turbulent) experiments and Turner (1963) measured 0·4–0·5 (turbulent case).

What is rather surprising is the large variation in the Reynolds number over the range of approximate similarity (figure 8). The shape of the curve is similar to that of the $y^2/\Delta t$ curve since $Re \equiv d/\nu\, dy/dt$, but $d/y = c$, a constant, so that

$$Re = \frac{c}{\nu} y \frac{dy}{dt} = \frac{c}{2\nu} \frac{dy^2}{dt} \rightarrow \frac{c}{2} \frac{y^2}{\Delta t}.$$

Because the maximum diameter of the thermal was as much as one-quarter of the tank width, a check was made on the effect of the container's walls. A tank double the size of the one normally used was built and several runs were performed. The uncertainty caused by different ambient densities (described previously) prevented precise determination of the wall effect. However, it was established that the effect on the thermal's displacement was less than 2% and the resulting $y^2/\Delta t$ curve was essentially the same as those in figure 4.

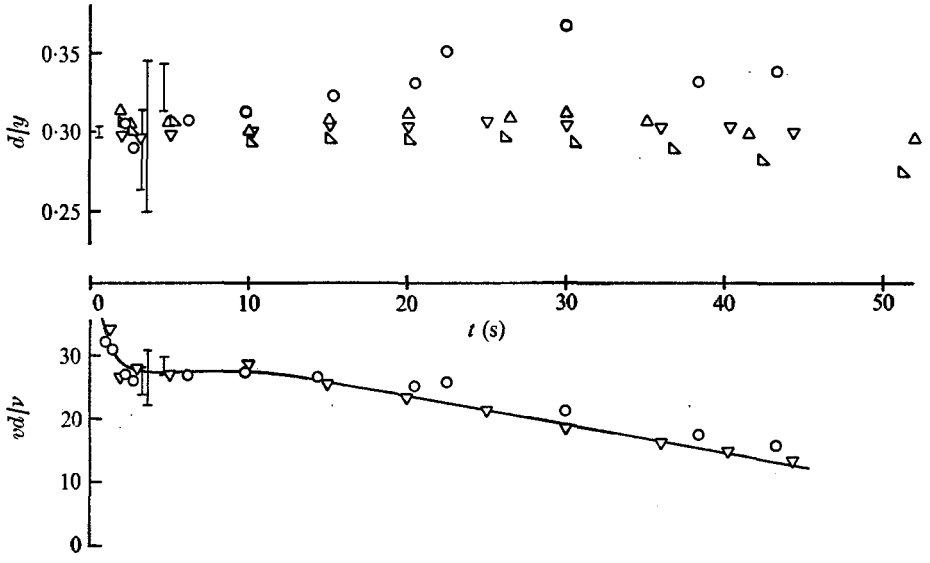

FIGURE 8. Reynolds number and d/y. $A_m = 9600$. ○, photos; △, run 1704*B*; ▽, run 1704*C*; ⧋, run 1704*D*.

No check was made on the effect of injecting the heat from a finite-sized source rather than a true point source but a 'point' source on a large plane will be discussed elsewhere. (The thermal's diameter at the onset of convection was approximately five times the electrode diameter.) This could impose an extra length scale on the experiment and thus could have, for example, an effect on the plot of the displacement as a function of A_m (figure 5).

6. Conclusions

The formation and growth of an isolated thermal vortex ring with a Reynolds number approximately equal to 25 has been described. Similarity was only approximate as demonstrated by the variation of the ratio $y^2/\Delta t$. Likewise, a deviation from geometric similarity was observed although the ratio d/y was constant to within the data scatter. By varying the amount of heat injected, the effect of changes in Rayleigh number on the displacement was observed.

The novel technique of operating essentially a conductivity probe at relatively large power to inject heat into a liquid with a minimum of disturbance has been demonstrated. Further uses of the technique will be reported elsewhere. These include more detailed measurements of the thermal formation, the effect of solid boundaries, motion of a sequential pair and a chain of thermals, plumes, evaporative convection and boiling.

We should like to acknowledge the help of the faculty, staff and graduate students at U.B.C. In particular, Mr Ervin Szabo designed and built the switching circuit, Mr Umesh Achia helped with the apparatus design and the photography, and Mr Larry Fish helped to run some experiments. This work was

supported by NRC grant no. A4936. Some data were reduced and the manuscript was prepared at the University of Tel-Aviv with support from the AFOSR(NAM), project no. 9781–01, and from the Center for Immigrant Absorption in Science, grant no. 8889.

Note added in proof. A better explanation than that given in the text for large time deviation from similarity might be the accumulated effect of energy dissipation since the assumed similarity form $y \propto \Delta t^{\frac{1}{2}}$ is possible only when the dissipation terms are neglected in the energy equation.

Taylor's (1946) 'entrainment' coefficient α (ratio of inflow velocity to thermal convection velocity) was calculated from the data to be 0·38. If the maximum cross-sectional area (rather than the area bounded by the core) is used in the calculation, $\alpha = 0{\cdot}28$. In addition to this 'entrainment' assumption, some authors assume the thermal to be spherical in shape and thus obtain the result $\alpha = d/2y$. The experimental value of $d/2y$ is 0·15, considerably different from the above α values.

REFERENCES

BATCHELOR, G. K. 1954 Heat convection and buoyancy effects in fluids. *Quart. J. Roy. Met. Soc.* **80**, 339–358.

CHU, T. Y. & GOLDSTEIN, R. J. 1973 Turbulent convection in a horizontal layer of water. *J. Fluid Mech.* **60**, 141–159.

ELDER, J. W. 1967 Transient convection in a porous medium. *J. Fluid Mech.* **27**, 609–623.

ELDER, J. W. 1968 The unstable thermal interface. *J. Fluid Mech.* **32**, 69–96.

ELDER, J. W. 1969 Hybrid computer techniques in the laboratory and classroom. *Phys. Fluids Suppl.* **12**, II 270–275.

ESCUDIER, M. P. & MAXWORTHY, T. 1973 On the motion of turbulent thermals. *J. Fluid Mech.* **61**, 541–552.

FOHL, T. 1968 Turbulent effects in the formation of buoyant vortex rings. *J. Appl. Phys.* **38**, 4097–4098.

FOX, D. G. 1972 Numerical simulation of three-dimensional, shape-preserving convective elements. *J. Atmos. Sci.* **29**, 322–341.

GIBSON, C. H. & SCHWARZ, W. H. 1963 Detection of conductivity fluctuations in a turbulent flow field. *J. Fluid Mech.* **16**, 357–364.

LILLY, D. K. 1962 On the numerical simulation of buoyant convection. *Tellus*, **14**, 148–172.

LILLY, D. K. 1964 Numerical solutions for the shape-preserving two-dimensional thermal convection element. *J. Atmos. Sci.* **21**, 83–98.

LIN, S.-C., TSANG, L. & WANG, C. P. 1972 Temperature field structure in strongly heated buoyant thermals. *Phys. Fluids*, **15**, 2118–2128.

MALKUS, J. S. & WITT, G. 1959 The evolution of a convective element: a numerical calculation. In *The Atmosphere and the Sea in Motion*, pp. 425–439. New York: Rockefeller Institute Press.

MAXWORTHY, T. 1972 The structure and stability of vortex rings. *J. Fluid Mech.* **51**, 15–32.

MORTON, B. R. 1960 Weak thermal vortex rings. *J. Fluid. Mech* **9**, 107–118.

MORTON, B. R., TAYLOR, G. I. & TURNER, J. S. 1956 Turbulent gravitational convection from maintained and instantaneous sources. *Proc. Roy. Soc.* A **234**, 1–23.

OGURA, Y. 1962 Convection of isolated masses of a buoyant fluid: a numerical calculation. *J. Atmos. Sci.* **19**, 492–502.

OKABE, J. & INOUE, S. 1961 The generation of vortex rings. *Rep. Res. Inst. Appl. Mech., Kyushu University*, **8**, 32.

RICHARDS, J. M. 1961 An experimental investigation of penetrative convection in the atmosphere, using a water model. Ph.D. dissertation, Imperial College, London.

RICHARDS, J. M. 1963 Experiments on motions of isolated cylindrical thermals through unstratified surroundings. *Int. J. Air Water Pollution*, **7**, 17–34.

SCORER, R. S. 1957 Experiments on convection of isolated masses of buoyant fluid. *J. Fluid Mech.* **2**, 583–594.

SPARROW, E. M., HUSAR, R. B. & GOLDSTEIN, R. J. 1970 Observations and other characteristics of thermals. *J. Fluid Mech.* **41**, 793–800.

TANKIN, R. S. & FARHADIEH, R. 1971 Effects of thermal convection currents on formation of ice. *Int. J. Heat Mass Transfer*, **14**, 953–961.

TAYLOR, G. I. 1946 Dynamics of a mass of hot gas rising in air. *U.S. Atomic Energy Commission Rep.* MDDC–919.

THOMPSON, D. W. 1970 Effect of interfacial mobility on mass transfer in gas–liquid systems. *Indust. Engng Chem. Fund.* **9**, 243–248.

TURNER, J. S. 1957 Buoyant vortex rings. *Proc. Roy. Soc.* A **239**, 61–75.

TURNER, J. S. 1963 Model experiments relating to thermals with increasing buoyancy. *Quart. J. Roy. Met. Soc.* **89**, 62–74.

TURNER, J. S. 1964 The dynamics of spheroidal masses of buoyant fluid. *J. Fluid Mech.* **19**, 481–490.

WANG, C. P. 1971 Motion of an isolated buoyant thermal. *Phys. Fluids*, **14**, 1643–1647.

WEGENER, P. P. & PARLANGE, J. Y. 1973 Spherical-cap bubbles. *Ann. Rev. Fluid Mech.* **5**, 79–100.

WOODWARD, B. 1959 The motion in and around isolated thermals. *Quart. J. Roy. Met. Soc.* **85**, 144–151

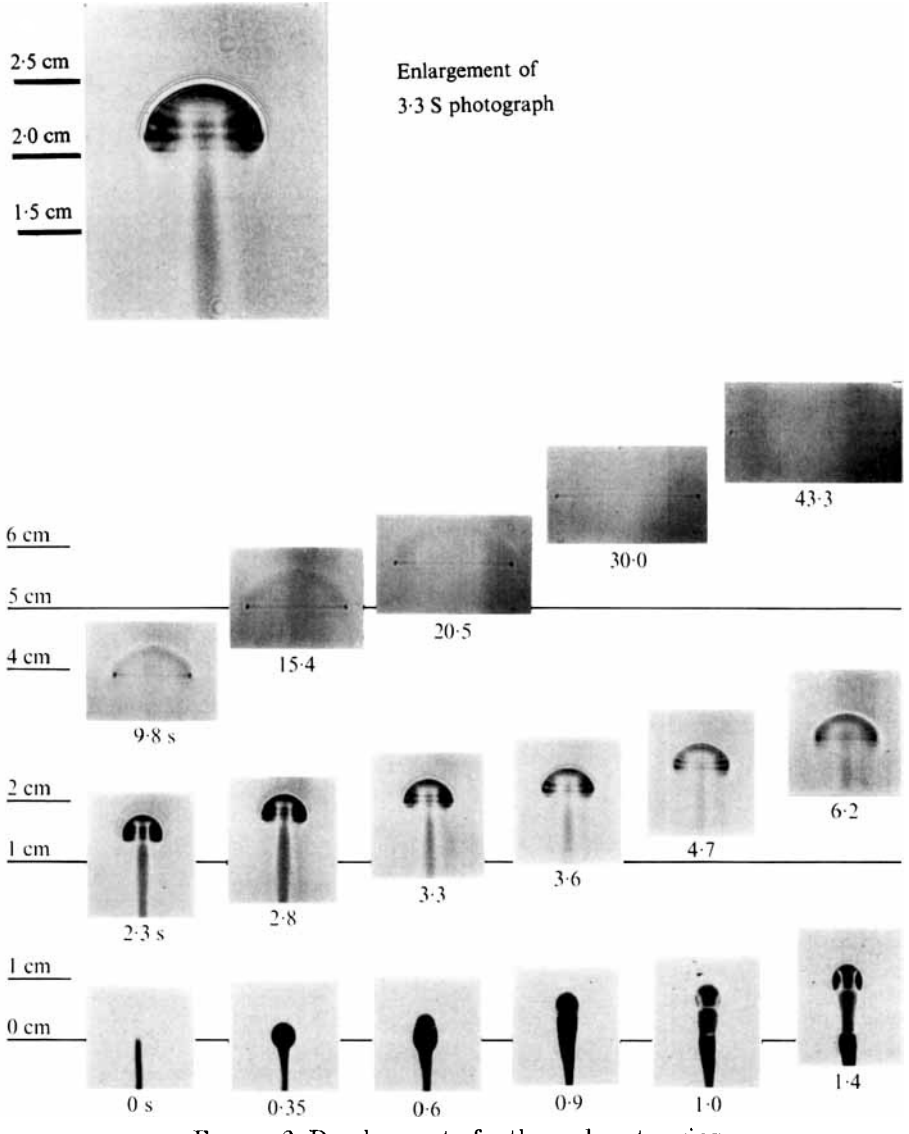

FIGURE 2. Development of a thermal vortex ring.